SDC-92-354

SDC
SOLENOIDAL DETECTOR NOTES

ESTIMATES OF THE NEUTRON FLUENCE FOR THE SDC DETECTOR

November 20, 1992

P.K. Job and L.E. Price
Argonne National Laboratory

T. Handler
University of Tennessee

T.A. Gabriel
Oak Ridge National Laboratory

ANL-HEP-TR-92-112
SDC-92-354

Estimates of Neutron Fluence for the SDC Detector [1]

P.K. Job and L.E.Price

Argonne National Lab, Argonne IL 60439

T. Handler

University of Tennessee, Knoxville TN 37996

T.A. Gabriel

Oak Ridge National Lab, Oak Ridge, TN 37831

1. Introduction

The high energy and high luminosity of SSC cause radiation problems to detectors. Almost all the radiation in the SDC detector[1] comes from the 20 TeV on 20 Tev pp collisions. The design luminosity corresponds to 10^8 collisions per second. This luminosity is maintained for 10^7 seconds (one SSC year). It is important to know the radiation fields experienced by the tracking volume, calorimeter, electronics and the phototubes. The loss of light due to the radiation damage to the scintillators can adversely affect the physics performance of the calorimeter. Studies have been carried out earlier to estimate the radiation dose in the SDC detector[2][3][4]. In this note we use ISAJET[5] in combination with CALOR89[6] to make an accurate prediction of neutron fluence at the various locations of the SDC detector. The low energy neutron fluence is important because of their large activation cross sections. In CALOR89 the low energy neutron fluence is accurately estimated by MORSE code[7].

2. Calculational Method

CALOR89 was interfaced with ISAJET modifying the CALOR subroutine SORS. Figure.1 gives a schematic diagram of the code system. The output particle data

[1]Work supported in part by US Department of Energy, Contract No. W-31-109-ENG-38, No. DE-AC05-84OR21400 and No. DE-AS05-ER03956

produced by ISAJET from 20 TeV pp collisions is read by the subroutine SORS to HETC[8]. The particle production from ISAJET has taken into account only the minimum bias events. Inorder to cut down the computational time the combinatorial geometry subroutines of HETC were replaced by the cylindrical geometry subroutines. The output from HETC is analysed by SPECT, which collected information on neutrons of energy $\geq$ 20 MeV and by MORSE which further transports the neutrons of energy $\leq$ 20 MeV through the detector. The neutron spectrum $\geq$ 20 MeV was calculated in 45 energy intervals between 20 MeV to 100 GeV. The neutron spectrum $\leq$ 20 MeV was calculated in MORSE in 103 energy intervals. MORSE code simulates all major and minor neutronic interactions, with the materials using an experimental cross section data base. There is no lower energy cutoff in MORSE. Neutrons are transported through the medium until they reach the thermal energy. The π^0 produced in the shower are ignored since it has been shown earlier that the neutron flux from an electromagnetic shower is an order of magnitude lower than the neutron flux from a hadronic shower[9][10].

3. Configuration for Calculations

The detector has been modelled as successive cylindrical configurations around the collision axis. The tracking volume, the coil, the barrel electromagnetic and hadronic calorimeters, the endcap electromagnetic and hadronic calorimeters and the forward calorimeter are simulated. The electromagnetic calorimeter is 4mm lead/4mm scintillator plates followed by the two separate hadronic sections. The HACI is 23.95 mm iron/4mm scintillator and HACII is 53.90mm iron/4mm scintillator[1]. Since the neutron mean free paths are large, each of these sections were homogenized conserving the material atom density. Figure.2 gives the schematic of the simulated configuration without the forward calorimeter. The shower max detector gap is not simulated separately. The forward calorimeter is assumed to be of iron with hydrogenous sampling material.

The cylindrical configuration is divided into 24 radial and 40 axial intervals. This provides 960 separate meshes (locations) at which neutron fluxes are calculated. The flux at a given location is estimated by dividing the sum of neutron track lengths by the mesh volume. At each of the location the neutron spectrum is also available for 148 energy intervals.

4. Results and Discussion

The summary results of these calculations are given in Table II. The results are also shown in figure.3. The flux and fluence values integrated over the energy range of $\geq$20 MeV and $\leq$20 MeV at specific locations of the detector are given. It can be seen that the high energy neutron flux ($\geq$20 MeV) at every location of the detector is an order of magnitude smaller than the low energy neutron flux. The maximum low energy neutron fluence is experienced by the front edge of the forward calorimeter. The tracking volume experience a neutron fluence of 1.88×10^{12}neutrons/cm^2/year. The neutron fluence at the endcap edge is ten times larger than that at the tracking volume. The neutron fluence at the back of the hadronic calorimeter is 5.5×10^{10}neutrons/cm^2/year. A complete flux map at 960 locations of the detector are also available.

These results are averages of one hundred ISAJET events. A total of 1757 particles are passed on to HETC. The statistical errors on these flux numbers are less than 5%. However some systematic errors of unknown magnitude are present in these results. We do not consider the rare interactions of interest to physicists from ISAJET, but only the "minimum bias events" which will occur 10^{15} times a year. This seems to be a reasonable assumption. However there are uncertainties in particle production and in the distribution of particles as a function of η (pseudorapidity) which is inherent in particle production codes. Comparisons with other particle production codes like PYTHIA[11] and DTUJET[12] are underway. The optimised ESKALE value[13] is used in HETC which may not introduce an error $\geq$1.5% for low energy particles($\leq$15GeV). The homogenization of individual sections may also have introduced a small error in particle production profile.

Conclusions

CALOR89 in combination with ISAJET can make reasonable predictions of neutron fluences in the SDC detector. These predictions are not alarmingly higher than the earlier conservative rough estimates. However the greatest uncertainty in these estimates are in the particle production profile as a function of pseudorapidity in the minimum bias events. Fine tuning of this function will add considerable accuracy into these calculations. The correct estimates of neutron fluences can lead to a more accurate prediction of the activation products and the resultant radiation dose rates.

References

[1]. SDC Technical Design Report, SSCL-SR 1215(1992).

[2]. D.E.Groom, Radiation Levels in the SSC Interaction Regions, SSC-SR-1033 (1988).

[3]. D.E.Groom, Radiation Levels in the SSC Detectors, SSC-201(1989).

[4]. J.D.Jackson, SSC Environmental Radiation Shielding, SSC-SR-1026(1987).

[5]. F.E.Page and S.D.Protopopescu, ISAJET, Snowmass CO (1986).

[6] T.A.Gabriel et al.,CALOR, ORNL/TM 5619(1977).

[7]. M.B.Emmett and N.M.Greene, Morse Code System, ORNL/TM-3706(1973).

[8]. T.W.Armstrong and K.C.Chandler,HETC Code, Nucl.Sci and Engg.49(1972)110.

[9]. G.Bathow et al.,Measurements of 6.3 GeV Electromagnetic Cascades and Cascade Produced Neutrons, Nuclear Physics B2(1967) 669.

[10]. J.Ranft and W.R.Nelson, Hadron Cascades Induced by Electron and Photon Beams in the GeV Energy Range, Nucl.Instr.Meth.A257(1987)177.

[11]. H.U.Bengtsson and T.Sjostrand, The lund Monte Carlo Code Pythia, LU TP 87-3 (19870.

[12]. J.Ranft et al., SSC Central Design Group Report, SSC 149(1987).

[13]. P.K.Job et al.,Comparison of CALOR89 Model Predictions with Scintillator plate Calorimeter Data, Nucl.Instr.Meth.,A309(1991)60.

Table I

Summary Results of Neutron Fluence for the SDC Detector

Detector Location		Neutron Flux 10^8 pp /colli./sec (neut/cm^2/sec)	Neutron Fluence 10^7 sec/year (neut/cm^2/year)
Tracking Volume (average)	≤ 20 MeV ≥ 20 MeV	1.85×10^5 3.00×10^3	1.85×10^{12} 3.00×10^{10}
Endcap (edge)	≤ 20 MeV ≥ 20 MeV	1.60×10^6 5.05×10^4	1.60×10^{13} 5.05×10^{11}
Forward Calorimeter	≤ 20 MeV ≥ 20 MeV	3.60×10^8 2.00×10^7	3.60×10^{15} 2.00×10^{14}
At the Back of Barrel Calorimeter	≤ 20 MeV ≥ 20 MeV	5.00×10^3 5.00×10^2	5.00×10^{10} 5.00×10^9

List of Figures

Figure.1 Schematic Diagram of the Code System

Figure.2 Schematic Diagram of the Simulated Configuration

(The Forward Calorimeter is not shown)

Figure.3 Summary Results of Neutron Flux for the SDC Detector

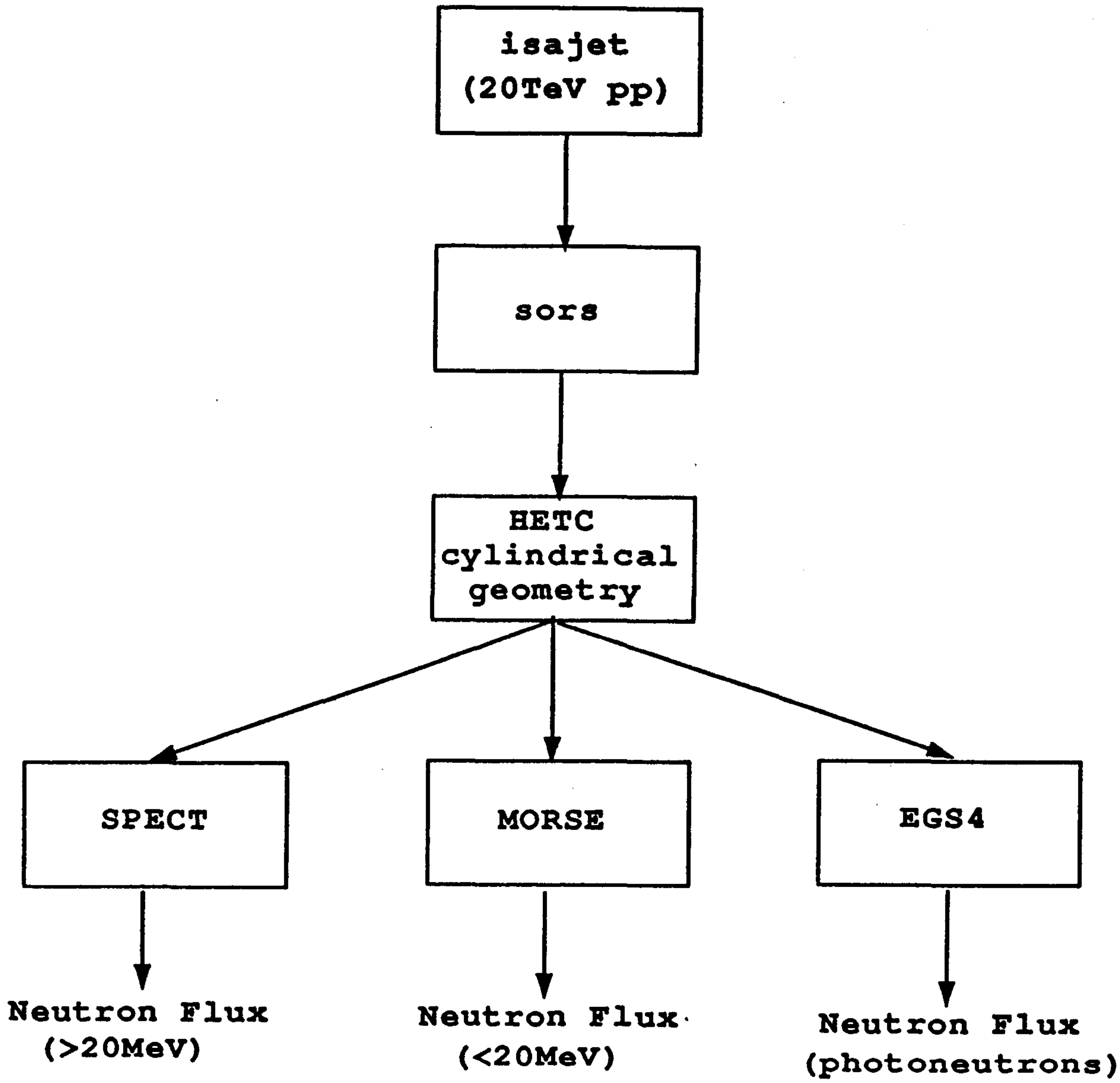
isajet
(20TeV pp)
sors
HETC
cylindrical
geometry
SPECT
MORSE
EGS4
Neutron Flux
(>20MeV)
Neutron Flux
(<20MeV)
Neutron Flux
(photoneutrons)

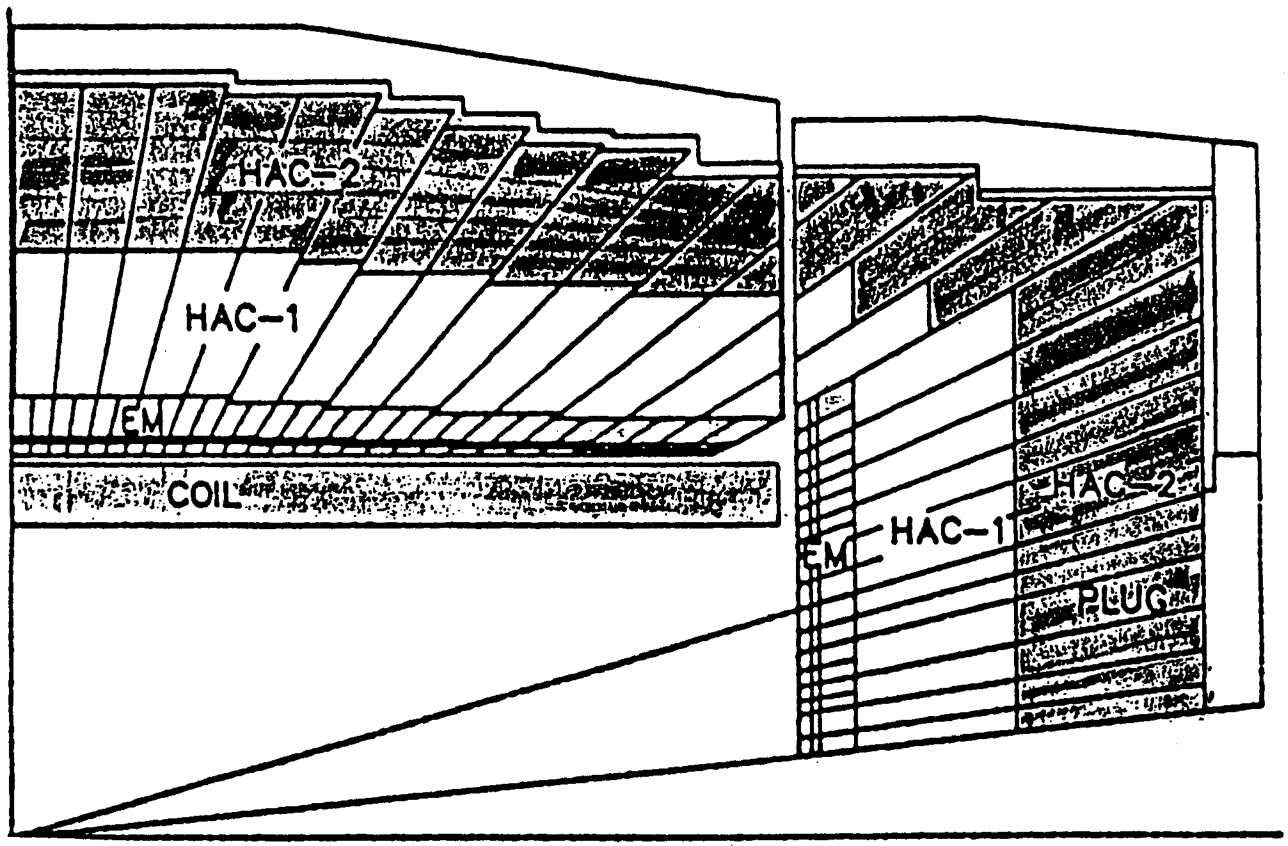
HAC-2
HAC-1
EM
COIL
EM
HAC-1
HAC-2
PLUG

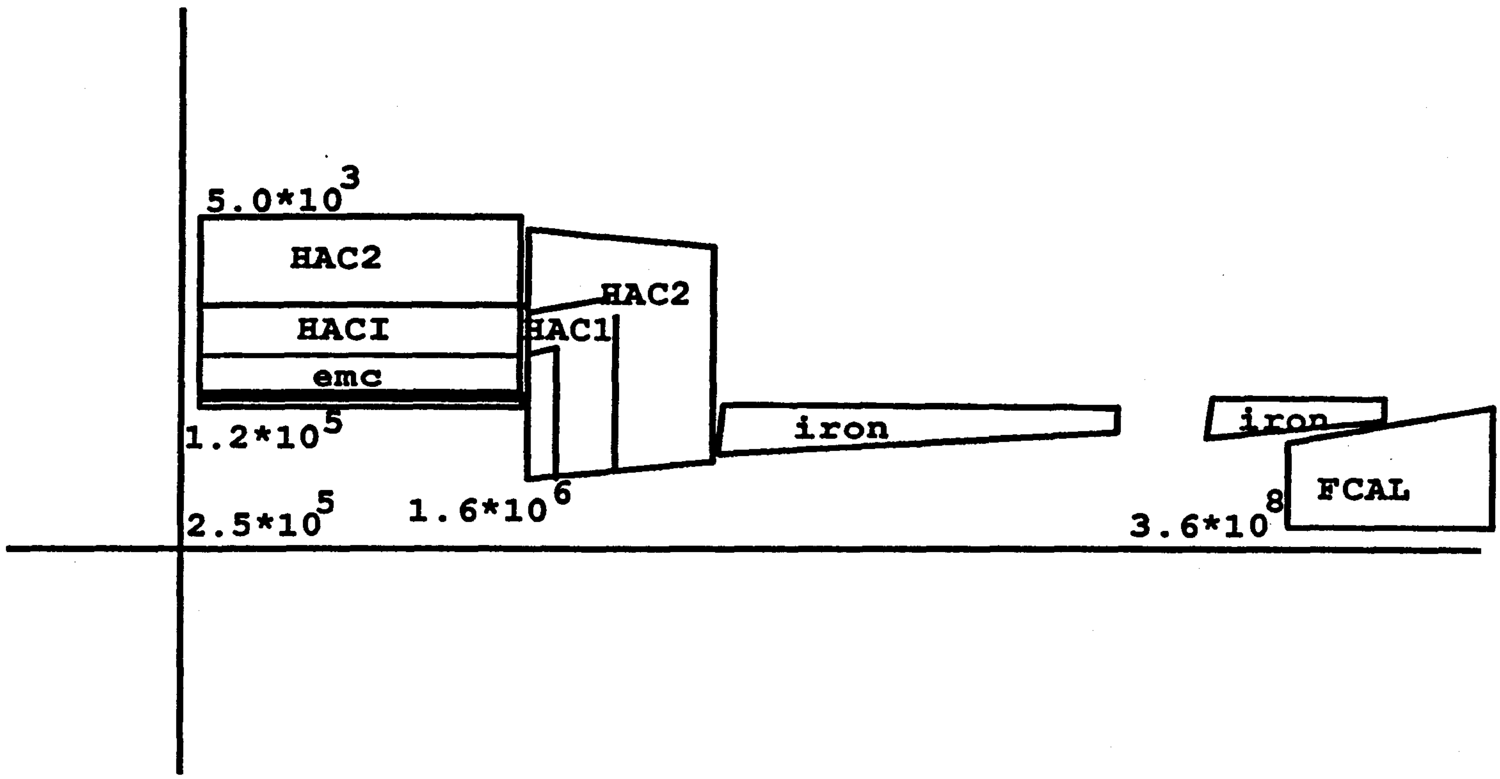

Neutron Flux in neutrons/cm^2/sec